1994-09

Testing the iron hypothesis in ecosystems of the equatorial Pacific Ocean

Martin, J.H.

Nature, Volume 371, 8 September 1994, pp. 123-129.
http://hdl.handle.net/10945/43402

Testing the iron hypothesis in ecosystems of the equatorial Pacific Ocean

J. H. Martin*, K. H. Coale†‡, K. S. Johnson†**, S. E. Fitzwater†, R. M. Gordon†, S. J. Tanner†, C. N. Hunter†, V. A. Elrod†, J. L. Nowicki†, T. L. Coley†, R. T. Barber§, S. Lindley§, A. J. Watson‖, K. Van Scoy‖, C. S. Law‖, M. I. Liddicoat‖, R. Ling‖, T. Stanton¶, J. Stockel¶, C. Collins¶, A. Anderson¶, R. Bidigare#, M. Ondrusek#, M. Latasa#, F. J. Millero☆, K. Lee☆, W. Yao☆, J. Z. Zhang☆, G. Friederich**, C. Sakamoto**, F. Chavez**, K. Buck**, Z. Kolber††, R. Greene††, P. Falkowski††, S. W. Chisholm‡‡, F. Hoge§§, R. Swift§§, J. Yungel§§, S. Turner‖‖, P. Nightingale‖‖, A. Hatton‖‖, P. Liss‖‖ & N. W. Tindale¶¶

† Moss Landing Marine Laboratories, PO Box 450, Moss Landing, California 95039-0450, USA
§ Duke University Marine Laboratory, Beaufort, North Carolina 28516, USA
‖ Plymouth Marine Laboratory, Prospect Place, Plymouth PL1 3DH, UK
¶ Naval Postgraduate School, Monterey, California 93943-5000, USA
# Department of Oceanography, University of Hawaii, 1000 Pope Road, Honolulu, Hawaii 96822, USA
☆ Rosenstiel School of Marine and Atmospheric Sciences, University of Miami, 4600 Rickenbacker Causeway, Miami, Florida 33149-1098, USA
** Monterey Bay Aquarium Research Institute, 160 Central Avenue, Pacific Grove, California 93950, USA
†† Oceanic and Atmospheric Sciences Division, Brookhaven National Laboratories, Upton, New York 11973, USA
‡‡ Ralph Parsons Laboratory, Department of Civil and Environmental Engineering, Massachusetts Institute of Technology, Cambridge, Massachusetts 02139, USA
§§ NASA/GFSC, Wallops Flight Facility, Building N-159, Wallops Island, Virginia 23337, USA
‖‖ School of Environmental Sciences, University of East Anglia, Norwich NR4 7TJ, UK
¶¶ Department of Meteorology, Texas A&M University, College Station, Texas 77843-3150, USA

The idea that iron might limit phytoplankton growth in large regions of the ocean has been tested by enriching an area of 64 km^2 in the open equatorial Pacific Ocean with iron. This resulted in a doubling of plant biomass, a threefold increase in chlorophyll and a fourfold increase in plant production. Similar increases were found in a chlorophyll-rich plume downstream of the Galapagos Islands, which was naturally enriched in iron. These findings indicate that iron limitation can control rates of phytoplankton productivity and biomass in the ocean.

Over 20% of the world's open ocean surface waters are replete with light and the major plant nutrients (nitrate, phosphate and silicate), yet standing stocks of phytoplankton remain low. The factors that limit phytoplankton growth and biomass in these high-nitrate, low-chlorophyll (HNLC) areas have been vigorously debated[1], but not resolved. The suggestion that increased phytoplankton production in HNLC areas could remove significant amounts of carbon dioxide from the atmosphere has renewed interest in this topic[2].

In some HNLC areas, it has been suggested that zooplankton grazing may contribute to the maintenance of low chlorophyll levels[3]. Strong turbulence at high latitudes may also mix phytoplankton below the critical depth, resulting in light-limitation of growth[4,5]. We believe that in addition to these factors, micronutrient elements, such as iron, which are important catalytic components in a wide variety of electron transport and enzymatic systems, have the potential to limit phytoplankton production in HNLC areas[6]. There are several lines of evidence in support of this notion.

The development of trace-metal clean sampling techniques over the last two decades has revolutionized our understanding of trace-metal biogeochemistry in the oceans[7]. Open-ocean iron concentrations in surface waters exist at picomolar (10^{-12} M) levels. These concentrations may be insufficient to support high phytoplankton biomass or maximum growth rates[8]. Addition of Fe to uncontaminated seawater samples has been shown to stimulate the growth of phytoplankton, especially diatoms[9–16]. Laboratory experiments have demonstrated that low iron levels may limit phytoplankton growth rates[17–19]. Moreover, techniques such as fast repetition rate (FRR) fluorometry have shown that photochemical energy-conversion efficiency is less than maximal in the equatorial Pacific and can be increased significantly in phytoplankton supplied with nanomolar (10^{-9} M) levels of iron[20,21]. These experiments suggest iron availability may regulate ocean production in HNLC areas.

The extrapolation of results from shipboard and laboratory incubation experiments to whole ecosystems has, however, been strongly criticized[22–24]. Although small-scale experiments may accurately reflect *in situ* processes occurring at the chemical or first trophic level, bottle experiments, by design, do not accurately represent the nature or scale of the community response. Studies of nutrient limitation in lakes have demonstrated that

* Deceased.
‡ To whom correspondence should be addressed.

incubations performed on small phytoplankton samples cannot easily be extrapolated to whole ecosystems. Mesocosm experiments with complete communities however, correlated highly with whole-lake responses to nutrient enrichments[25].

We believe that the effects of iron on phytoplankton growth in HNLC areas can be more confidently resolved by mesoscale enrichments of whole ecosystems[26]. Until recently however, enrichment experiments in the open ocean have not been feasible due to the difficulties in tracking a patch over time. The recent development of technology to measure ultra-trace concentrations of the inert gas sulphur hexafluoride, SF_6, has made it possible to mark a patch of sea water and track it for long

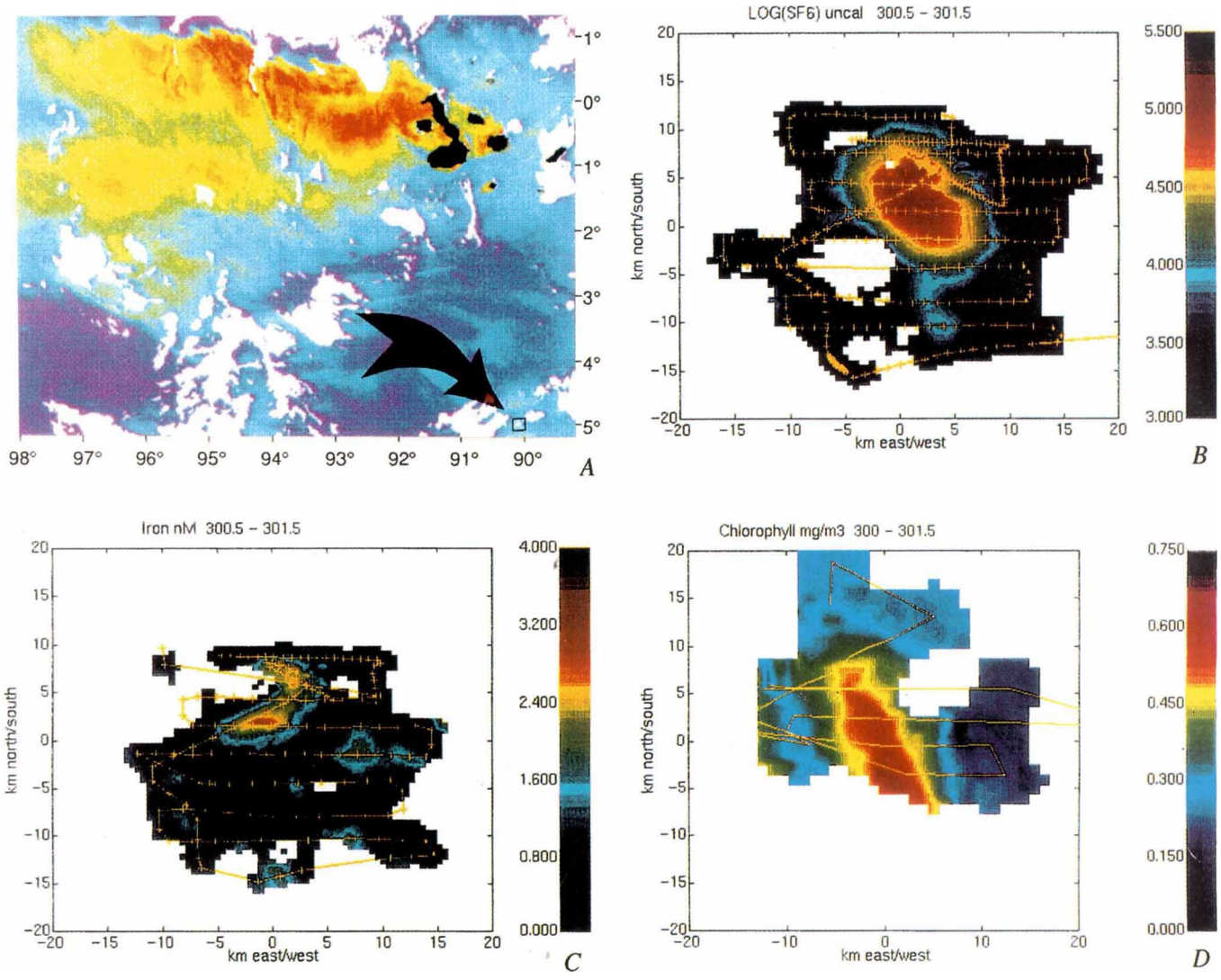

FIG. 1 *A*, False-colour image of the study site from the Coastal Zone Colour Scanner on the Nimbus 7 satellite, October 1983. This image indicates the chlorophyll-rich plume extending west of the Galapagos Islands (red colour indicates higher chlorophyll concentrations; image courtesy of G. Feldman). The arrow indicates the location and relative size of the study site at 5° S. *B–D*, Contour plots of the concentrations of SF_6, (*B*) YD 300.5–301.5, iron (*C*) YD 300.5–301.5, and chlorophyll *a* (*D*) YD 300–301. All parameters in *B–D* are plotted relative to the GPS buoy which served as the centre of a lagrangian frame of reference used during the first part of the experiment. A total volume of 15,600 l of the iron solution (8,100 mol or 450 kg Fe) was dispensed. The SF_6 solution was prepared by dissolving 0.35 mol of SF_6 in sea water in a 2,300-l steel tank before departure from Miami. The SF_6 was pumped (1.4 l min^{-1}) together with the iron solution (12 l min^{-1}) into the propellor wash as the ship steamed at ~9 km h^{-1}. The ship's track was updated every 5 min relative to the central GPS buoy (see below) to correct for horizontal advection during the 24-h deployment. This strategy was estimated to produce an increase in the iron concentration within the 35-m mixed layer of 3.8 nM and an SF_6 concentration of 180 fM (ref. 51). Horizontal eddy diffusion was predicted to horizontally homogenize the streaks within 1 d of mixing, whereas overturn of the mixed layer would vertically homogenize the iron and SF_6 concentrations every evening[36]. The GPS buoy was interrogated every 5 min to determine the location of the ship relative to this central point. In addition, four WOCE drifter buoys equipped with ARGOS position transmitters were deployed at each corner of the patch. Updates of the ARGOS buoy positions could be received four times a day. All of the buoys were attached to holey sock drogues set at 10 m to reduce wind slippage relative to the enriched patch. A flow-through pumping system with an intake set at 3 m on the ship's bow was used to sample surface sea water. SF_6 measurements using electron-capture gas chromatography were used to determine the position of the enriched iron patch, relative to the GPS buoy. This information was used daily to correct the central lagrangian reference point based on the GPS buoy (that is, correction for buoy slippage). Surface sea water was supplied for iron analyses via an all-Teflon pumping system also with the intake on the ships' bow. Samples were acidified in-line (pH 3) before analyses resulting in the detection of dissolved iron, freshly precipitated colloidal iron, and much of the aged, colloidal iron (total dissolvable iron, DFe). DFe was analysed continuously using both colorimetric and chemiluminescent techniques (detection limit, 0.3 nM). Chlorophyll depicted in *D* represents that filtered and extracted from discrete samples taken along the ship's track. Chlorophyll concentrations were quantified using standard fluorescence techniques on board ship.

periods of time[27,28]. Thus, when combined with iron enrichment, the SF_6 tracer provides the potential to assess ecosystem level responses to added iron[29].

The region south of the Galapagos Islands was proposed as the most favourable place for such an iron-enrichment experiment[30]. In this paper, we report the initial results of a mesoscale iron-enrichment experiment performed in this area of the equatorial Pacific. Additionally, the waters both upstream and downstream of the Galapagos Islands were studied to further evaluate the potential role of iron in regulating production. We found substantial and convincing evidence to indicate that iron additions to these HNLC regions increases phytoplankton productivity and biomass.

Open ocean iron fertilization experiment

In mid-October 1993, the RV *Columbus Iselin* occupied an area approximately 500 km south of the Galapagos Islands to begin the enrichment experiment (Fig. 1*A*). Ambient iron concentrations in this area were of the order of 0.06 nM (ref. 31). An area of about 64 km^2 was enriched with iron to a concentration of

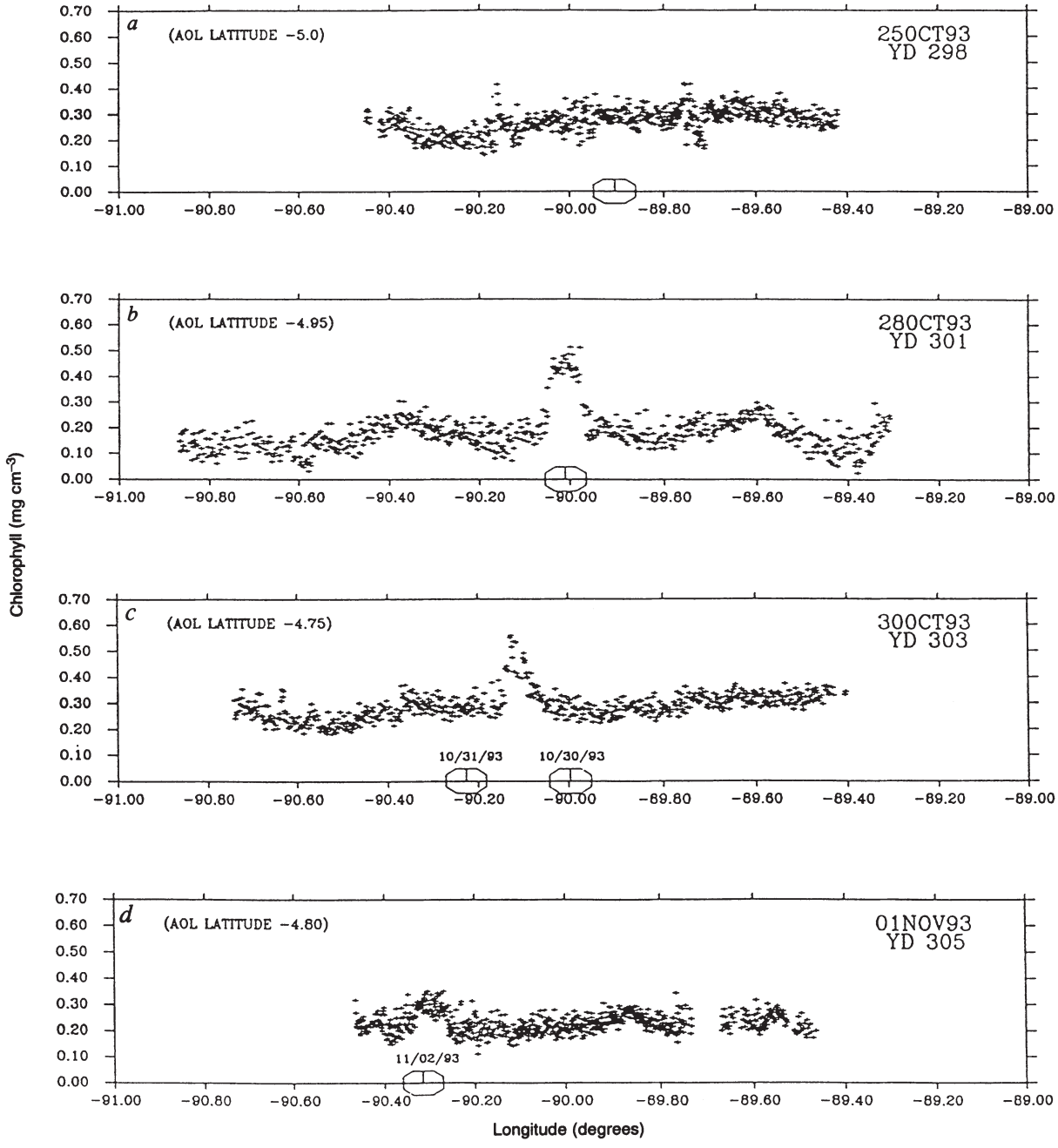

FIG. 2 *a–d*, The NASA airborne oceanographic LIDAR flown in a P-3 Orion aircraft (from Goddard Space Flight Center/Wallops Flight Facility) provided pigment measurements determined by laser-induced chlorophyll fluorescence on YD 298 (*a*), YD 301 (*b*), YD 303 (*c*) and YD 305 (*d*). For each mission day a single representative east–west flightline was selected from numerous lines flown over the patch. The latitude of the horizontal flightline is given in each panel. The longitude of the most contemporaneous central buoy position is indicated by the circle and date at the bottom of each panel. The flight legs were ~180 km long and were flown in a star pattern centred on the GPS buoy[52]. The surface manifestation of the patch was seen at (or very near) the buoy positions on each day after the initial deployment on YD 298. Fluorescence signals showed a rapid initial response followed by a decay in signal strength as the experiment progressed. This result is consistent with the measurements of iron and photochemical energy conversion efficiency[42].

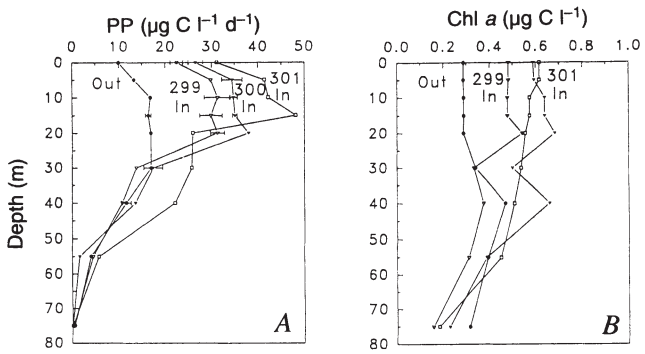

FIG. 3 Vertical profiles, for the 3 days following fertilization, of primary production, PP, (*A*) chlorophyll *a* concentrations, Chl *a*, (*B*) as a function of time inside and outside the patch. Outside values are depicted for YD 299. Primary production was measured using $H^{14}CO_3^-$ uptake determined at various light levels, in incubations on board the ship. Chlorophyll was determined from filtered and extracted samples as in Fig. 1*D*. The errors associated with the chlorophyll analyses are generally <0.02 μg C l^{-1}. The depth to which the water column was enriched was ~35 m up to YD 301 (just before subduction). It is in the upper 35 m that the differences are most pronounced. Productivity and chlorophyll both converge by 75 m.

~4 nM. Iron at this level, in bottle experiments, is sufficient to cause large increases in chlorophyll and complete depletion of the available major nutrients within 5 to 7 days. The enriched patch was tracked for 10 days and monitored for changes in biological, chemical and physical parameters.

To ensure that changes in properties within the patch could be attributed to the presence of iron and not to natural variation of the area in general, the study area was surveyed on year days (YD) 295 to YD 297 to determine its biological, chemical and physical heterogeneity. The initial survey, as well as later stations outside the patch, showed mixed-layer plant nutrient concentrations of nitrate, phosphate, silicate and ammonium to be 10.8 ± 0.4 μM, 0.92 ± 0.02 μM, 3.9 ± 0.1 μM and 0.21 ± 0.02 μM respectively, with a chlorophyll concentration of 0.24 ± 0.02 μg l^{-1}. These values are typical of the equatorial HNLC region[32,33]. The low-chlorophyll conditions were substantiated throughout the region by overflights of the NASA airborne oceanographic lidar (AOL) optical laboratory before the experiment (Fig. 2). Iron (450 kg) was added to the patch as a 0.5 M Fe(II) solution in sea water at approximately pH 2, together with 0.35 mol of the inert chemical tracer, SF_6.

Four tracking strategies were employed to maintain contact with the iron enriched area. (1) The iron deployment and initial sampling were performed about a central lagrangian reference point located by a drogued buoy equipped with a Global Positioning System (GPS) receiver interfaced to a VHF packet radio transmitter and receiver. (2) SF_6 was released in constant ratio to the iron injected into the patch. This inert tracer was monitored continuously with detection limits of less than 10^{-16} M. (3) The NASA AOL conducted overflights on YD 298, YD 301,YD 303 and YD 305 to assess the large-scale effects of iron on surface-water chlorophyll in the patch as compared to the surrounding region (Fig. 2). (4) The concentration of iron in the patch was determined continuously throughout the experiment[34,35].

The patch was sampled from YD 298.9 to YD 302.0 using surface pumping systems as the ship steamed through the study area. Each day, one major hydrographic station was occupied within the patch and one outside the patch at a time near local noon. Samples were collected at these stations for analysis of primary productivity, species composition, chlorophyll, FRR fluorescence, pigments (by high-pressure liquid chromatography), nutrients, particulate organic carbon (POC), particulate organic nitrogen (PON), dissolved organic carbon (DOC), dimethylsulphide (DMS), dimethylsulphoniopropionate (DMSP), dissolved and particulate trace metals and halocarbons as well as hydrographic and CO_2 system parameters. The concentration of the SF_6 tracer, together with the ship's position relative to the GPS buoy, were used to distinguish stations inside the patch from those outside.

Physical behaviour of the patch. The physical coherence of the patch was one of the greatest concerns in performing the experiment. One potential problem was that as the patch spread by turbulent diffusion, it would disperse into long streaks as it crossed eddy or frontal boundaries. It was, however, remarkably stable. As predicted, the added iron and SF_6 were distributed rapidly throughout the mixed layer by horizontal eddy diffusion and convective overturn. The patch remained as an intact unit from YD 298 to at least YD 302, expanding to become a rectangle of approximately 8 × 12 km.

Late on YD 302 the core of the patch was subducted beneath a low-salinity front to a depth of 30–35 m, where it was confined in a 5–10 m layer at the top of the thermocline. The patch was still detectable after its subduction by the SF_6 signal, the distinct salinity and low light transmission[36]. SF_6 concentrations did not decrease after subduction. The highest values of SF_6 found each day were a constant 40–50 fM (femtomolar, 10^{-15} M) over the entire 9-day duration of the experiment. The constancy of the SF_6 concentration suggests that unfertilized waters did not penetrate into the core of the patch even after subduction.

Iron chemistry. Dissolvable iron concentrations (DFe) as high as 6.2 nM were measured in the core of the patch within 4 hours of fertilization. DFe decreased rapidly on the first day due to night-time convective mixing of the water column, with the highest values on the subsequent day being 3.6 nM, in good agree-

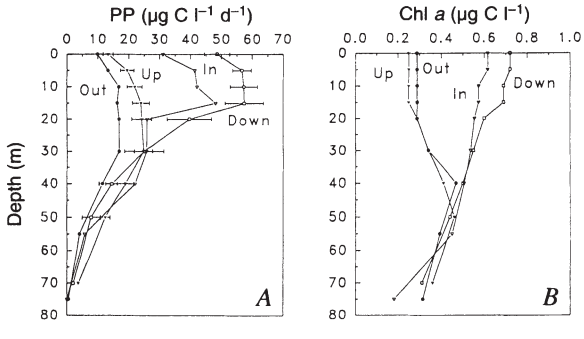

FIG. 4 Comparison of vertical profiles of primary production (*A*) and chlorophyll *a* concentrations (*B*) for stations inside and outside the fertilized patch, and stations upstream (westward) of the Galapagos Islands and downstream (eastward) of the Galapagos Islands.

ment with predicted concentrations (3.8 nM Fe). Concentrations of DFe in the core of the patch decreased ~15% each day. Despite this decrease, contour plots of iron and SF_6 in the surface layer were still in good spatial agreement on YD 301, 3 days after fertilization (Fig. 1*B*, *C*). Iron dropped below our detection limit (0.3 nM) in the subducted layer by YD 303.

Previous studies indicate that three distinct pools of iron were formed on injection; dissolved Fe(III), colloidal Fe(III) and cellular Fe. Most of the Fe(II) injected into the patch was oxidized within minutes to Fe(III)[37] and colloidal iron oxyhydroxides should have precipitated with a first-order rate constant of 0.1 h^{-1} (ref. 16). Biological uptake of the dissolved Fe(III) proceeded rapidly (see below). Of the three iron forms, colloidal Fe(III), especially when aged, is not thought to be bioavailable. Laboratory experiments, however, indicate that these colloids would remain suspended in the surface waters (K.H.C. *et al.*, unpublished observations) where they could be photoreduced and rendered bioavailable[16,38]. A computer model of iron photochemistry[16] suggests that once the patch was subducted, there would be insufficient light to maintain the bioavailable pool of dissolved Fe(III) at concentrations above our shipboard detection limits.

Chemical response. Nutrient measurements indicated little or no systematic difference in nitrate, phosphate and silicate concentrations within the mixed layer between inside and outside stations. The ratio of nitrate uptake to chlorophyll production in Fe incubation experiments is approximately 1 mol NO_3 per g chlorophyll (ref. 6). Thus a chlorophyll increase of 0.5 μg l^{-1} should have been accompanied by a 0.5 μM decrease in nitrate. Because initial nitrate concentrations were 10.8 μM and the day-to-day variance in the nitrate measurements was 0.4 μM (1σ) a 0.5 μM decrease would have been at our limit of detection. Phosphate and silicate also showed no definitive change over this time period inside the patch.

Ammonium, however, showed a consistent difference between inside and outside stations. After fertilization, the mean ammonium concentrations measured inside the patch from YD 299 to YD 302 were 0.10 ± 0.07 μM (95% confidence interval) lower than the values observed outside the patch. An ammonium maximum with values near 0.45 μM was regularly found near the base of the mixed layer outside the patch. This maximum decreased within the fertilized patch and, with one exception, no ammonium concentrations higher than 0.12 μM were found inside the patch. Preferential uptake of ammonium[39] (especially by the picoplankton, the primary ammonium utilizers) would be expected as physiological rates increased.

The measurements of CO_2 fugacity and total CO_2 in the patch were significantly lower than those observed outside the patch[40]. These changes were apparent within 2 days of the iron release and are lower than expected, but consistent with the drawdown in major plant nutrients. Particulate DMSP, integrated throughout the water column, showed a significant increase (50–80%) in the fertilized patch. DMSP is produced by phytoplankton and decays to produce DMS[41]. There were no clear changes in DMS concentration in surface waters ($2.5 \text{ nM} \pm 0.4$), which is not surprising considering the duration of the study compared to the time needed to degrade DMSP to DMS. Preliminary analysis of low-molecular-weight halocarbon data suggests that there was some increase in the concentration of methyl iodide inside the patch relative to outside stations.

Biological response. Biological parameters measured outside the patch during the course of the experiment remained similar to those measured within the patch region before the addition of Fe. Photosynthetic energy conversion efficiency (relative fluorescence) was the first biological response detected[42] after Fe addition. Relative fluorescence dramatically increased by the first sampling transect through the patch, indicating a large physiological response within the first 24 hours (the period required to fertilize the patch)[42].

Maximum primary production values in the mixed layer were initially 10–15 μg C l^{-1} d^{-1} (R.B., personal communication). After fertilization, productivity increased monotonically to values of 48 μg C l^{-1} d^{-1} on YD 301 (Fig. 3*A*). This 3–4 times increase in productivity was observed in all size fractions indicating an overall enhancement of rates in both small and large phytoplankton. Chlorophyll increased nearly three-fold by YD 301 from 0.24 μg l^{-1} to maxima consistently over 0.65 μg l^{-1} (Figs 2, 3*B*). NASA overflights confirmed the increase in chlorophyll using Lidar laser fluorescence measurements of the surface layer (Fig. 2).

Preliminary microscopic examination of water collected within the patch indicated an increase in biomass in all classes counted (cyanobacteria and protists). Total autotrophic biomass (excluding Prochlorophytes) calculated from cell numbers and volumes[43–45], increased from 16 to 33 μg C l^{-1}. The largest contributors to the plankton biomass were *Synechococcus*, red fluorescing picoplankton and autotrophic dinoflagellates. Diatoms were a small fraction of the total plankton biomass (17%) yet showed increases similar to other groups. Heterotrophic biomass increased from 4.7 to 7.3 μg C l^{-1} and was dominated by heterotrophic dinoflagellates and ciliates. Prochlorophytes were not counted microscopically but preliminary flow cytometric analyses indicate little difference in cell numbers between stations inside and outside the patch.

Galapagos plume study

Satellite imagery collected with the Coastal Zone Colour Scanner on the Nimbus 7 satellite shows a plume of high-chlorophyll water that is found regularly to the west of the Galapagos Islands in association with the nutrient-rich, westerly flowing, south equatorial current[46] (Fig. 1*A*). Hydrographic surveys also have shown anomalously high chlorophyll concentrations and depleted nitrate concentrations over the Galapagos platform and downstream (westward) of the islands[47]. It has been suggested

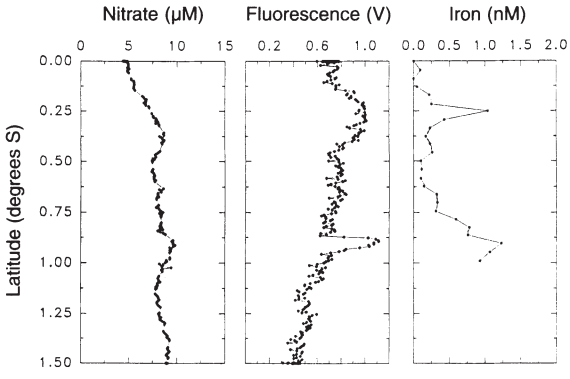

FIG. 5 Nitrate concentration, fluorescence intensity and iron concentrations as a function of latitude on a surface-water transect, along 90° 45′ W, from 1° 30′ S to the Equator.

that these elevated chlorophyll levels are the result of iron derived from the island platform[47], but metal distributions in the Galapagos region are unknown. A series of stations were, therefore, occupied both upstream (to the east) and downstream (to the west) of the Galapagos Islands. Detailed trace-metal profiles were determined, as well as onboard analyses of the same parameters measured in the patch study. Surface-water iron, nitrate, CO_2 fugacity and fluorescence were also measured on transits between stations. The purpose of this sampling strategy was to determine if detectable anomalies of iron were present and, if so, their relationship to increased levels of chlorophyll and primary production in the downstream plume.

Survey results. The Galapagos Islands lie near a sharp equatorial front that separates low-nutrient, oligotrophic waters to the north from high-nutrient waters to the south. There are strong horizontal gradients as a result. Waters immediately around the Islands, during our survey, had nitrate concentrations greater than 10 μM at the surface. Chlorophyll concentrations and rates of primary production were significantly elevated at stations downstream, when compared to upstream (eastward, Fig. 4).

Surface-water iron concentrations were about 0.06 nM upstream of the Islands. Iron concentrations as high as 1.3 nM were detected on a transect across the downstream plume, from 1° 30′ S to 0° along 91° 45′ W (Fig. 5). These high concentrations appeared to be associated with upwelled water that was in contact with the shelf and has higher salinity and lower temperature than the surrounding surface water masses. Elevated chlorophyll fluorescence signals were also associated with the high iron concentrations (Fig. 5). The highest iron concentrations (3 nM) were found between the islands of Isabella and Fernandina. These concentrations were associated with chlorophyll levels in excess of 13 μg l^{-1}, near-maximum relative fluorescence and nearly complete depletion of nitrate.

Extracted surface chlorophyll concentrations in the downstream plume were typically near 0.7 μg l^{-1}, which is about 3 times higher than in the upstream water mass (Fig. 4*B*). However, large increases in chlorophyll fluorescence signals, which are indicative of even higher chlorophyll concentrations, were recorded by the shipboard fluorometer and the aircraft Lidar system on the downstream meridional transects through the plume[38,48]. These high fluorescence signals were regularly associated with frontal features characterized by lower temperatures, higher salinities and higher nitrate concentrations. The highest fluorescence signals always occurred at the interface between these upwelled water masses and the surrounding water. Particulate DMSP and DMSO levels were also significantly higher in the plume than at stations upstream, whereas differences in DMS levels were small.

Discussion

Our results demonstrate a direct and unequivocal biological response of the equatorial Pacific ecosystem to added iron. The response observed in the fertilization experiment was similar in magnitude and character to the increased production and chlorophyll found in the Galapagos plume. Until this study, there were no measured differences in chemical constituents which could explain higher biomass west of the islands. The presence of elevated concentrations of iron in the downstream plume is consistent with the hypothesis that the high chlorophyll concentrations are supported by iron, originating from the Galapagos platform.

Concentrations of chlorophyll as well as rates of primary productivity were up to a factor of 3–4 higher in both the patch and the downstream plume compared to outside the patch and upstream of the islands. The rapid increase in photosynthetic energy conversion efficiency in all size classes of phytoplankton in the patch confirm that at least some members of the natural phytoplankton populations are physiologically limited by lack of available iron[42]. Chlorophyll-specific rates of primary production showed a smaller change. These rates of primary production are less sensitive to iron availability because the carbon/chlorophyll ratio changes on the addition of iron. Moreover, laboratory studies show a three-fold increase in the carbon/chlorophyll ratio as cells become Fe-limited[20]. Carbon/chlorophyll ratios (wt/wt) in the patch decreased from an initial value of 54 to 38 by YD 300. Productivity on a per unit carbon basis, as determined by estimates of cell biovolume, indicate an initial doubling time of 1.0 d^{-1}. By YD 301 the doubling time was 1.5 d^{-1}, a 50% increase. This indicates that the cells grow faster on a per unit carbon basis when iron is present.

Dimethylsulphoniopropionate in the particulate phase also increased within the patch relative to waters outside the patch. This compound serves an osmoregulatory function (or possibly as a cryoprotectant) in certain classes of phytoplankton. It degrades to DMS, a volatile sulphur-containing gas that contributes to non-seasalt sulphur in the atmosphere. The production of these compounds in the iron-enriched patch is consistent with the ice-core record, which links greater iron availability to increased phytoplankton production during glacial times[49].

There was evidence for increased grazing within the fertilized patch. Microscopic examination of samples collected inside and outside the patch indicate that microheterotrophic biomass increased by ~50% over the course of the patch experiment. This increase was rapid and appeared to level off quickly. The corresponding average increase in grazing pressure (assuming grazing rate (μg C d^{-1}) = 2.5 × heterotrophic biomass; F.C. and K.B., personal communication), was approximately 4.5 μg C l^{-1} d^{-1}.

The biomass increase (excluding Prochlorophytes), estimated from microscopic counts of cell numbers and volumes, was 16.4 μg C l^{-1} (a doubling). If the pool of inorganic carbon decreased by an equivalent amount, then the fugacity of CO_2 in the mixed layer should have decreased by about 3 μatm in the fertilized patch. This finding is low but consistent with the measurements of Watson and co-workers, indicating that some carbon may have been exported or converted to DOC[40]. When the increased effects of grazing are considered, the gross biomass increase must have been about 60 μg C l^{-1}. Most of this increase (43 μg C l^{-1}) was consumed over the 9-day experiment by grazers. These values are conservative in that they exclude consideration of mesozooplankton grazing. Qualitative observations of filters and plankton tows suggest that the mesozooplankton also increased, which presumably occurred when vertically migrating plankton encountered the high biomass in the patch and remained there to feed.

All biological indicators confirmed an increased rate of phytoplankton production in response to the addition of iron. The geochemical effect of iron enrichment was, however, small in both studies relative to the biogeochemical effect that could have been achieved if all the major nutrients were consumed. Nonetheless, the similarity in chlorophyll and productivity profiles measured between the fertilized patch and the downstream Galapagos plume suggests that similar mechanisms control the ecosystem response to added iron. There are several hypotheses that could explain why nutrients were not completely consumed and chlorophyll did not increase more dramatically. (1) Although iron did stimulate initial growth, the depletion of another micronutrient prevented further growth. (2) Grazing increased in the patch and plume environments as a result of increased production and the systems rapidly reached steady state. (3) Iron was lost from the system due to colloidal aggregation and/or sinking of larger particles containing iron.

First, we do not think that the limitation of the response to added iron results from the depletion of another trace nutrient. If that were the case, trace-metal clean shipboard incubations would not result in complete consumption of the major nutrients, but they do. Although there is no significant difference in dissolved Zn, Cu, Ni, Co or Cd between inside and outside stations, we cannot rule out the possibility that *in situ* growth resulted in the limitation of phytoplankton growth by other

bioactive trace metals due to biological uptake and re-partitioning of these resources. This possibility seems unlikely over these short timescales and the magnitude of the biological response.

Second, increased grazing pressure must have exerted some control on the rate of biomass increase. Yet grazing does not seem to be a likely mechanism for preventing phytoplankton from completely consuming the available major nutrients in the patch and downstream of the Galapagos Islands. Other investigators have also seen large depletions of major nutrients at stations over other regions of the Galapagos platform[47]. Although reduced grazing in bottle experiments is likely, there is no reason to expect an equivalent reduction in grazing pressure, especially by microheterotrophs, over shelf regions where high chlorophyll concentrations were observed.

Third, the available data suggest that nutrient consumption and phytoplankton growth is limited in the patch and downstream of the Galapagos Islands because of a loss term that occurs in open waters but not in bottles or in shallow shelf regions. This loss term might be sinking of larger phytoplankton. If sinking keeps the diatom population low, then the absolute rates of nutrient uptake will be limited because phytoplankton growth is a first-order process. Iron would also be lost much more rapidly from open ocean systems than from bottles or shallow waters. In shallow waters, sinking iron is trapped in a nepheloid layer near the bottom. Concentrations in the nepheloid layer along continental margins can be greater than 10 nM (ref. 8). Upwelling of iron-enriched water from a shallow nephloid layer will continually resupply the euphotic zone with iron. The biological similarity of shipboard iron enrichment experiments and stations over the Galapagos platform and Bolivar canal suggest that it is the elimination of the loss term for iron (that is, continuous supply of iron) that may be responsible for complete utilization of nutrients.

Vertical profiles of iron in the equatorial Pacific show a nutrient-like distribution with concentrations increasing at greater depth. However, the highest dissolved-iron values found in the equatorial Pacific (3° S, 140° W) are 0.55 nM at depths of 2,400 m (ref. 31). The depth of the source for upwelled water that reaches the surface along the equator is less than 150 m (ref. 50). Iron concentrations at this depth are less than 0.2 nM. Upwelling of water from the Equatorial undercurrent could not produce the large iron concentrations that we observed in the meridional transect and at the Bolivar canal, unless it is dramatically enriched by contact with the island platform. This must account for the iron concentrations greater than 1 nM observed near the Islands, and ocean currents are, therefore, the most plausible mechanism for the transport of island derived materials to the plume.

The residence time of bioavailable iron added to surface waters must be very short. Iron disappeared rapidly from the patch and was also not detected far from the presumed source downstream of the islands. This indicates that, within a given parcel of water, both the patch and plume systems reflect a transient addition of iron rather than a sustained addition, characteristic of bottle enrichments and shallow shelf stations. With a transient addition, only a few cell divisions are possible before the iron is removed from the system. Continual supply must occur to sustain production. This probably accounts for the low plateau that was reached in the biological response to the iron-addition experiment and the relaxation in relative fluorescence within the fertilized patch[42], but we cannot yet definitively rule out other factors.

We have shown that it is possible to enrich an area of the open ocean with iron and track it for many days. This capability can be used to conduct refined experiments that will address issues of grazing and iron loss, which will be coupled to continuous or semicontinuous enrichment experiments. Given the relatively cohesive nature of the patch that was produced, it seems possible to create and track even smaller patches and instrument these patches to obtain better estimates of carbon export. Open-ocean manipulative experiments are, therefore, possible and ecological studies in the open ocean are no longer limited to passive observations and bottle experiments. This, we feel, may change significantly the way geochemical and ecological studies are performed in the ocean.

Finally, we wish to make it clear that the purpose of these experiments is to understand the nature of the controls on productivity and ecosystem function in HNLC waters. Such experiments are not intended as preliminary steps to climate manipulation. We also emphasize the transient nature of these experiments which indicate that the impact of these manipulations is erased in a very short time, because of the short residence time of iron and the rapid food web response. □

Received 11 April; accepted 1 August 1994.

1. Chisholm, S. W. & Morel, F. M. M. (eds) *Limnol. Oceanogr.* **36** (1991).
2. Martin, J. H. *Paleoceanography* **5,** 1–13 (1990).
3. Frost, B. W. *Mar. Ecol. Prog. Ser.* **39,** 49–68 (1987).
4. El-Sayed, S. Z. *Comp. Biochem. Physiol.* **90B,** 489–498 (1988).
5. Mitchell, B. G., Brody, E. A., Holm-Hansen, O., McClain, C. & Bishop, J. *Limnol. Oceanogr.* **36,** 1662–1677 (1991).
6. Martin, J. H. & Fitzwater, S. E. *Nature* **331,** 341–343 (1989).
7. Bruland, K. W., Franks, R. P., Knauer, G. A. & Martin, J. H. *Analytica chim. Acta* **105,** 223–245 (1979).
8. Martin, J. H. & Gordon, R. M. *Deep-Sea Res.* **35,** 177–196 (1988).
9. Martin, J. H., Fitzwater, S. E. & Gordon, R. M. *Globl. Biogeochem. Cycles* **4,** 5–12 (1990).
10. Martin, J. H., Gordon, R. M. & Fitzwater, S. E. *Limnol. Oceanogr.* **36,** 1793–1802 (1991).
11. Coale, K. H. *Limnol. Oceanogr.* **36,** 1851–1864 (1991).
12. De Baar, H. J. W. *et al. Mar. Ecol. Prog. Ser.* **65,** 34–44 (1990).
13. Price, N. M., Anderson, L. F. & Morel, F. M. M. *Deep-Sea Res.* **38,** 1361–1378 (1991).
14. Ditullio, G. R., Hutchins, D. A. & Bruland, K. W. *Limnol. Oceanogr.* **38,** 495–508 (1993).
15. Hutchins, D. A., Ditullio, G. R. & Bruland, K. W. *Limnol. Oceanogr.* **38,** 1242–1255 (1993).
16. Johnson, K. S., Coale, K. H., Elrod, V. E. & Tindale, N. W. *Mar. Chem.* **46,** 319–334 (1994).
17. Sunda, W. G., Swift, D. G. & Huntstman, S. *Nature* **351,** 55–57 (1991).
18. Brand, L. E. *Limnol. Oceanogr.* **36,** 1756–1772 (1991).
19. Hudson, J. M. & Morel, F. M. M. *Limnol. Oceanogr.* **35,** 1002–1020 (1990).
20. Greene, R. M., Geider, R. J. & Falkowski, P. G. *Limnol. Oceanogr.* **36,** 1772–1782 (1991).
21. Greene, R. M., Kobler, Z. S., Swift, D. G., Tindale, N. W. & Falkowski, P. G. *Limnol. Oceanogr.* (in the press).
22. Banse, K. *Limnol. Oceanogr.* **35,** 772–775 (1990).
23. Dugdale, R. C. & Wilkerson, F. P. *Globl Biogeochem. Cycles* **4,** 13–19 (1990).
24. Frost, B. W. *Limnol. Oceanogr.* **36,** 1616–1630 (1991).
25. Hecky, R. E. & Kilham, P. *Limnol. Oceanogr.* **33,** 796–822 (1988).
26. Roberts, L. *Science* **253,** 1490–1491 (1991).
27. Upstill-Goddard, R. C., Watson, A. J., Wood, J. & Liddicot, M. I. *Analytica chim. Acta* **249,** 555–562 (1991).
28. Ledwell, J. R., Watson, A. J. & Law, C. S. *Nature* **364,** 701–703 (1993).
29. Watson, A. J., Liss, P. & Duce, R. *Limnol. Oceanogr.* **36,** 1960–1965 (1991).
30. Martin, J. & Chisholm, P. (eds) *US JGOFS Planning Report No.* 15 (US JGOFS Planning Off, Woods Hole Oceanographic Inst., Woods Hole, 1992).
31. Gordon, R. M., Coale, K. H. & Johnson, K. *EOS* **75,** 114, Abstr. (1994).
32. Chavez, F. P. & Barber, R. *Deep-Sea Res.* **34,** 1229–1243 (1987).
33. Fiedler, P. C., Philbrick, V. & Chavez, F. P. *Limnol. Oceanogr.* **36,** 1834–1850 (1991).
34. Elrod, V. A., Johnson, K. S. & Coale, K. H. *Analyt. Chem.* **63,** 893–898 (1991).
35. Coale, K. H., Blain, S. P., Fitzwater, S. E., Coley, T. L. & Johnson, K. S. *Deep-Sea Res.* (submitted).
36. Stanton, T. P. & Watson, A. J. *EOS* **75,** 134, Abstr. (1994).
37. Millero, F. J. & Sotolongo, S. *Geochim. cosmochim. Acta* **53,** 1867–1873 (1988).
38. Wells, M. L. & Mayer, L. M. *Deep-Sea Res.* **38,** 1379–1395 (1991).
39. Raymont, J. E. G. *Phytoplankton* (Pergamon, Oxford, 1980).
40. Watson, A. J. *et al. Nature* **371,** 143–145 (1994).
41. Keller, M. D., Bellows, W. K. & Guillard, R. R. L. in *Biogenic Sulfur in the Environment* (eds Saltzman, E. S. & Cooper, W. J.) 167–182 (Am. Chem. Society, Washington DC, 1989).
42. Kolber, Z. *et al. Nature* **371,** 145–149 (1994).
(this issue: update)
43. Waterbury, J., Watson, S., Valois, F. & Franks, D. *Can. Bull. Fish. aquat. Sci.* **214,** 71–120 (1985).
44. Eppley, R., Reid, F. & Strickland, J. *Bull. Scripps Inst. Oceanogr.* **17,** 33–42 (1970).
45. Beers, J. & Stewart, G. *Bull. Scripps Inst. Oceanogr.* **17,** 67–87 (1970).
46. Feldman, G. C. in *Tidal Mixing and Plankton Dynamics: Notes on Costal and Estuarine Studies* (eds Brown, J., Yentsch, M. & Peterson, W. T.) 77–106 (Springer, Berlin, 1986).
47. Chavez, F. P. & Brusca, R. C. in *Galapagos Marine Invertebrates* (ed. James, M. J.) 9–33 (Plenum, New York, 1991).
48. Sakamoto, C. M. & Friederich, G. *EOS* **75,** 150, Abstr. (1994).
49. Roger, T. & Wilson, S. *Atmos. Envir.* **22,** 2637–2638 (1988).
50. Gargett, H. E. *Limnol. Oceanogr.* **36,** 1527–1545 (1991).
51. Fitzwater, S. E. *et al. EOS* **75,** 150, Abstr. (1994).
52. Hoge, F. *et al. EOS* **75,** 134, Abstr. (1994).

ACKNOWLEDGEMENTS. K. Coale would like to acknowledge the leadership of Dr John H. Martin, whose vision and perseverance has forged this hypothesis and whose presence and humour we all miss dearly. He would have loved to see this project through. We thank M. Wells for his comments. This work was supported by the US Office of Naval Research and the US National Science Foundation.